NASA-CR-200969

Final Report
Attachment 2

October 17, 1995

CONTRACT NAS8-38856

Structural Damage Prediction and Analysis for Hypervelocity Impact

AIAA 92-1407 Space Debris Surfaces (Computer Code): Probability of No Penetration versus Impact Velocity and Obliquity.

Prepared for:
National Aeronautics and Space Administration
George C. Marshall Space Flight Center
Marshall Space Flight Center,
Alabama 35812

LOCKHEED MARTIN

MAF/MMA 31-100 (3/95)

AIAA

AIAA 92-1407

Space Debris Surfaces (Computer Code): Probability of No Penetration versus Impact Velocity and Obliquity

N. Elfer*, R. Meibaum*, and G. Olsen†
* Martin Marietta, New Orleans, LA
† NASA-Marshall Space Flight Center, Huntsville, AL

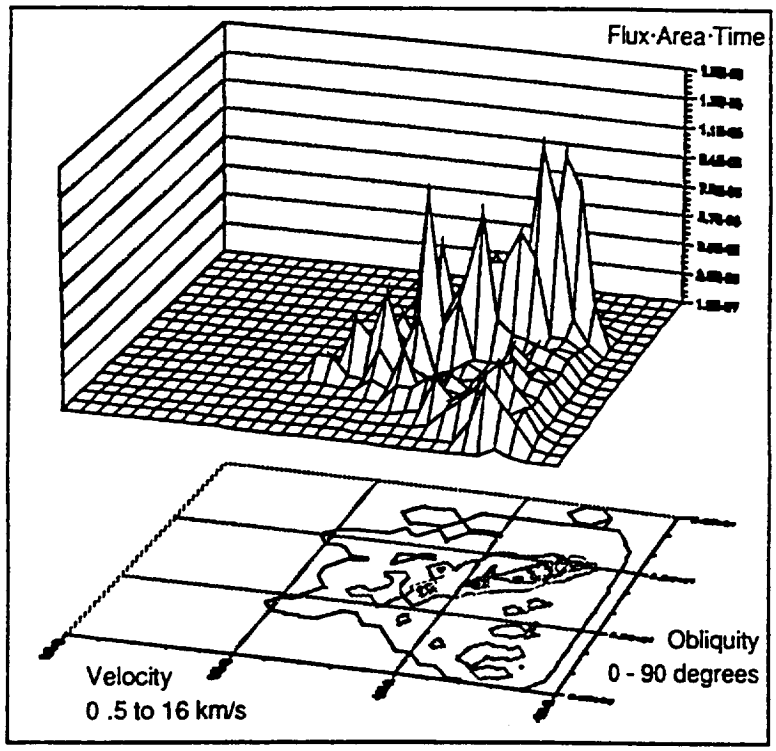

AIAA Space Programs and Technologies Conference
March 24-27, 1992 / Huntsville, AL

SPACE DEBRIS SURFACES:

N. Elfer*,†, R. Meibaum*, G. Olsen**,†

Abstract

A unique collection of computer codes, Space Debris Surfaces (SD_SURF), have been developed to assist in the design and analysis of space debris protection systems. SD_SURF calculates and summarizes a vehicle's vulnerability to space debris as a function of impact velocity and obliquity.

An SD_SURF analysis will show which velocities and obliquities are the most probable to cause a penetration. This determination can help

threat's impact velocity and obliquity, as described in the following sections. The output tells the designer which areas are most vulnerable.

Environment

The space debris environment is defined in terms of a flux of particles of diameter, d, or larger, dependant on the year of interest (due to assumed growth in the environment and solar flux variations) and the spacecraft altitude.[4] Figure 1 shows

spacecraft from more than approximately 10° above or below a plane tangent to the local Earth normal. Otherwise the debris would enter the Earth's atmosphere and be removed as a threat. Therefore, the relative impact velocity in LEO is determined by the orbital velocity, V_0, and the intersection angle, Ø, of the two orbits. The impact velocity, V_i, is:

$$V_i = 2\,V_0 \cdot \cos\left(\frac{180° - Ø}{2}\right)$$

Figure 2 shows the fraction of the total flux coming from angles relative to the direction of flight. The relative impact velocity for the intersection of 388 km orbits is also shown on the plot.

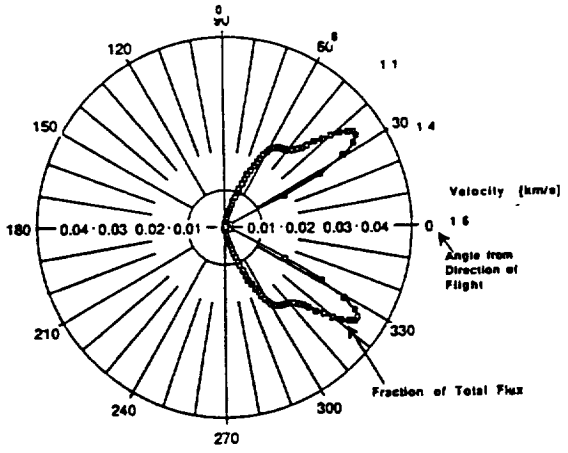

Fig. 2. Angular and velocity distribution of flux.

Ballistic Limit Surface

The spectrum of debris sizes, velocities, and obliquities that may impact a shield lead to a variety of penetration mechanisms. Figure 3 illustrates a ballistic limit surface for hypervelocity impact on a multiwall shield. A projectile diameter at a velocity and obliquity above the surface will penetrate the shield. A diameter below the surface will not penetrate the shield. There are several penetration mechanisms which are described in Fig. 3. Changes in shield parameters affect each penetration mechanism differently. Therefore, it is important for the designer to know what penetration mechanism has the greatest effect on the overall probability of no penetration.

Critical Damage

It is necessary to understand the consequences of a penetration. A small penetration should be avoided because of potential difficulties in finding and repairing a leak. However, a small penetration

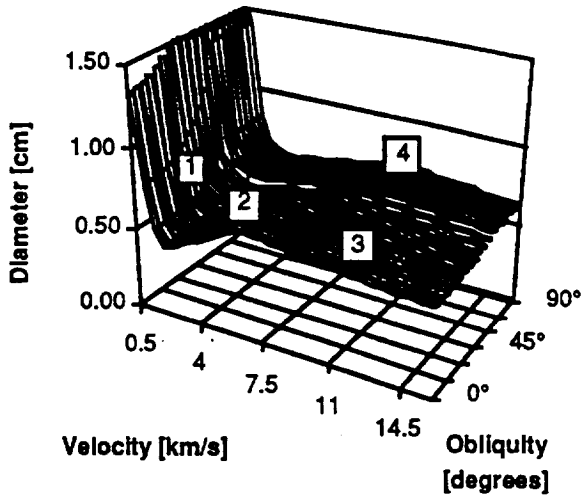

1 - Single particle penetration.
2 - Fragment penetration.
3 - Momentum failure by bulge or spall.
4 - Ricochet, bumper fragments penetrate.

Fig. 3. Ballistic Limit Surface with multiple penetration mechanisms.

does not result in an immediate fatality. Critical damage will be defined as penetrations resulting in rapid depressurization as well as catastrophic crack growth. There is a theoretical threat of bodily injury due to fragments, but this is much less likely and will not be treated in this paper.

For Space Station Freedom, the critical hole size for too rapid depressurization has been estimated as 10 cm in diameter. To get this diameter, either a large projectile or petalling of the hole is necessary. Conservative fracture analyses predict that large petals may lead to catastrophic

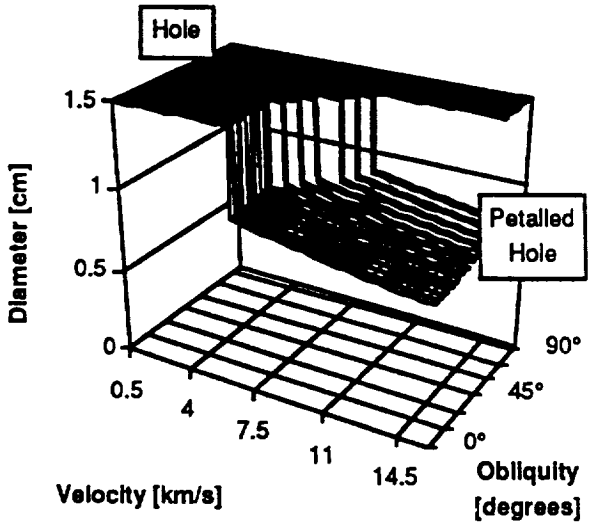

Fig. 4. Critical Damage Surfaces.

rupture rather than simple depressurization.

A critical damage limit surfaces is presented in Fig. 4. At high velocity there is sufficient intermediate thermal blanket/shield to prevent cratering or spall, and the rear wall fails by momentum induced bulging and petalling. This can open a hole or propagate a crack to a much larger size than the initial damage area. The projectile diameter to cause critical damage was estimated to be 50% larger than the projectile diameter to cause penetration. For low velocity penetration the projected area of the projectile, plus a damage zone, is assumed to control critical damage. This is a very rough assumption because there is insufficient data about the momentum deposited in the rear wall. The estimate of the size of the damage zone will not have a strong influence on the overall probability because of the large projectile size.

An alternative high-velocity penetration mechanism may be wide area spall. A larger particle would then be necessary to drive petalling and crack growth in the rear wall, because much of the momentum will be transferred to the spall fragment. To estimate the influence of this failure mechanism, the projectile diameter was assumed to be 225% of the ballistic limit diameter for the following calculations.

Probability Analysis

The probability of no penetration (PNP) from each direction and for each element is based on the Poisson distribution for zero events:

$$PNP_{el} = \exp\left(- \sum_{i=1}^{nthreats} (N_i \cdot A_i) \cdot t \right)$$

where (with consistent units)

- N_i = flux that penetrates from each threat direction, i,
  = $4 \cdot f_i \cdot N_r(d_i)$.
- N_r = flux on a randomly tumbling plate (specification definition) of diameter d or larger. d_i is the diameter to penetrate at the velocity and obliquity of the ith threat.
- f_i = fraction of flux from threat direction.

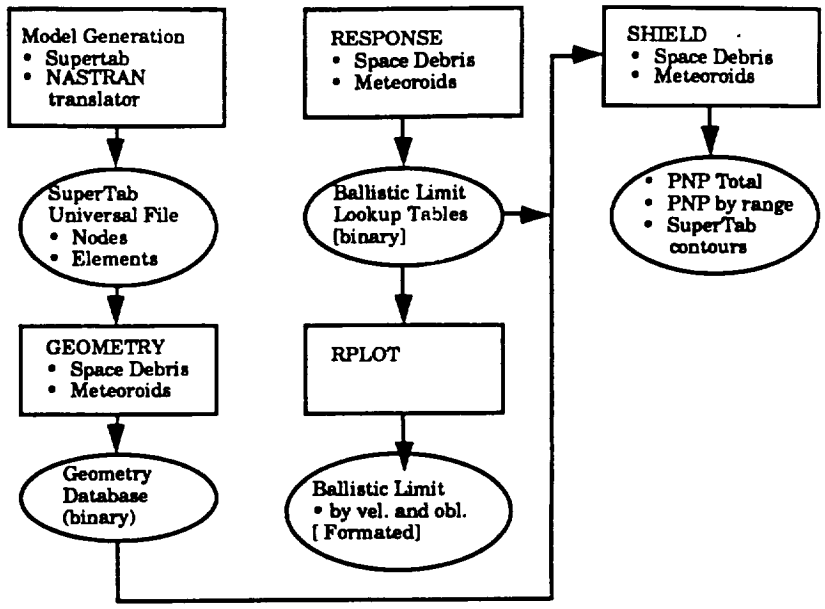

Fig. 5. BUMPERII Modules, Input and Output.

- A_i = projected area of the facet in the flux direction.
- t = exposure time.

The total PNP is determined by the product of the PNP for each element.

$$PNP_{total} = \prod_{j=1}^{nelements} PNP_j$$

Figure 5 shows the BUMPERII modules and their input and output as they calculate PNP. BUMPERII starts with a SuperTab output file finite element model of the spacecraft.

The GEOMETRY module of BUMPERII calculates the projected area of the elements exposed to each threat direction. A significant part of this calculation is intercomponent shadowing. This can be a very time consuming process for a large model.

The RESPONSE module creates a ballistic limit surface from a menu of user selected penetration equations. The ballistic limit for each shield of interest is stored in a matrix for every 0.25 km/s and 5° obliquity. This is also stored in binary form in the computer. Another BUMPERII code, RPLOT, reads the binary file and puts out a formatted file with the ballistic limit at 0°, 15°, 30°, 45°, and °60 obliquity for 2D plots.

The SHIELD module calculates the PNP for any range of element numbers requested by the analyst. SHIELD also has an option to create a SuperTab file to plot probability contours on the original geometry model.

SD_SURF Analysis Approach

To design the most effective shield, the analyst must know which penetration or damage mechanism is predominant. It is the goal of the SD_SURF computer programs to provide this information.

The flux associated with each point on the ballistic limit surface can be weighted by the probability of an impact at that particular velocity and obliquity.

$$PNP(V,\beta) = \exp[-N(d)\cdot A(V,\beta)\cdot t]$$

where $A(V,\beta)$ is the total area of the spacecraft that will be impacted at an obliquity, β, from a debris particle at velocity, V, and N(d) is the flux associated with the diameter d that just penetrates at V and β.

There is a difference in the PNP calculated for a unit area at a single velocity and obliquity versus distributing the area over two bracketing velocities and two bracketing obliquities. This is due to the non-linear relationship between flux and diameter. On the other hand, the analysis of a curved surface in BUMPERII is more accurate only if the size of the facets is smaller than the five-degree increments used on the RESPONSE and AREA SURFACE tables.

SD_SURF - FORTRAN Version

The interrelationship of the FORTRAN modules of SD_SURF is shown in Fig. 6. SD_SURF acts as a post-processor of BUMPERII-RESPONSE and GEOMETRY output. It provides additional information not readily obtainable from BUMPERII.

The A_SURF module reads the BUMPERII-GEOMETRY binary output to create the exposed area matrix as a function of velocity and obliquity. Rather than lump the area of one facet at the nearest velocity and obliquity, A_SURF uses the lever rule to distribute the projected area, for one

the flux·area·time (NAT) array. A text based contour map is generated, which should be compatible with any FORTRAN platform, and also a text file that may be used with sophisticated graphics packages. Examples of the contour plots will be shown in the examples in the next section of this paper.

The final FORTRAN module is R_PLOT5. It is used to translate BUMPERII-RESPONSE output files to text formatted files. The text formatted file is set up at 0.5 km/s and five-degree increments rather than the 0.25 km/s and five-degree increments used by RESPONSE. Commas are used as delimiters to ease import by the EXCEL modules.

SD_SURF - EXCEL 3.0 Version

The EXCEL version can be used both as an alternative or a complement to the FORTRAN version. The EXCEL version is not as fast or as "turnkey" as a FORTRAN application. However, it has the advantages of a spreadsheet: customized calculations and analyses are simple to generate; error checking is very easy; there is quick access to graphing.

The structure of the EXCEL version is shown in Fig . 7. The backbone of the PNP calculation is the PNP Template. There are several different

areas on the worksheet:

- Ballistic Limit surface, diameter to penetrate in increments of 0.5 km/s and five degrees of obliquity. (It is created on a Ballistic Limit Template or imported from RESPONSE via R_PLOT 5.)
- Environment definition including year, solar flux level (explicit or calculated), and altitude.
- Flux calculation for each diameter in the ballistic limit surface. (This is a function macro that is defined on the function macro worksheet.)
- Area Surface, $A(V,\beta)$, created using Area_Maker Macro, or imported from A_SURF.
- Flux · Area · Time, N·A·T, for each V and β. (The summation of these cells is used to

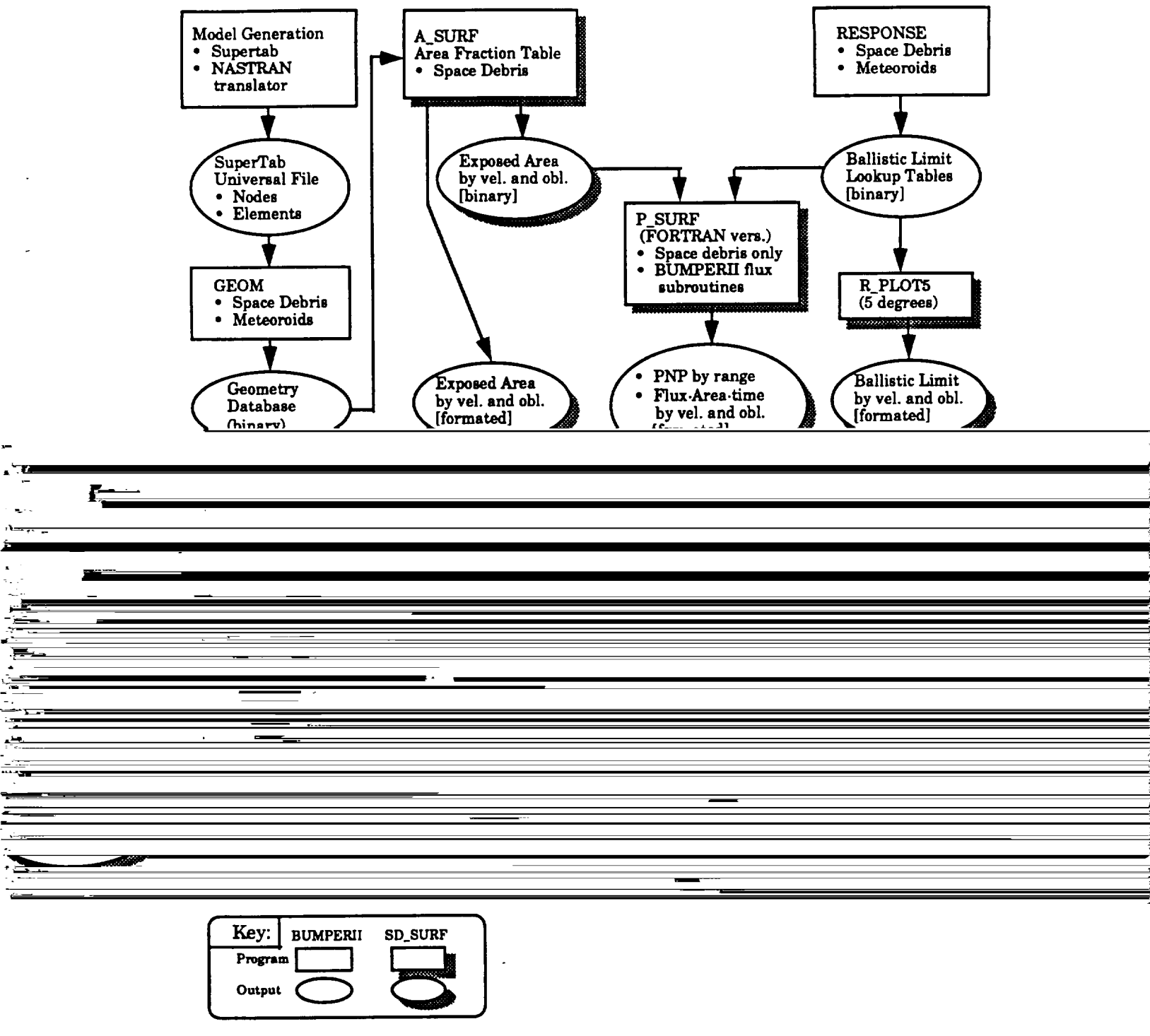

Fig. 6. SD_SURF - FORTRAN and BUMPERII Modules, Input and Output.

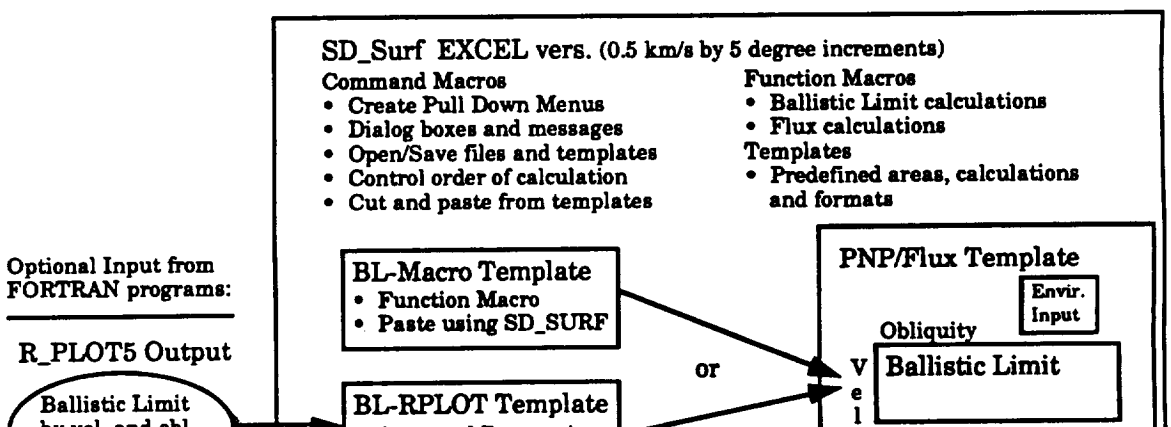

The Area Surface maybe created on the Area_Template using the Area_Maker Macro. The analyst selects the geometry desired from a pull-down menu. The standard geometries are shown in Fig. 8. The specific geometry is entered in customized dialog boxes. Each facet is analyzed at each velocity increment. This is effectively 64 threats (at equally spaced velocities), compared to the 45 threat default in BUMPERII.

SD_SURF for EXCEL lacks some of the features of BUMPERII. BUMPERII must be used for shadowing analysis in GEOMETRY, multiyear flux averaging in SHIELD, or the extensive iterations required to run PEN4 in RESPONSE. However, the GEOMETRY and RESPONSE output may be imported via the FORTRAN A_SURF and R_PLOT5 programs. Multiyear flux calculations can be programmed into the EXCEL macros with a corresponding increase in analysis time.

Probability Studies

Effective Area

The A_SURF program and the Area_Template calculate the effective exposed area at each velocity and obliquity. Figure 9 illustrates the analysis of a flat plate that is oriented edge on to the direction of flight (90 degrees yaw in Fig. 8). The first part of the analysis is the calculation of the projected area relative to each impact velocity direction. Figure 9 (b) shows the probability associated with each impact velocity. Figure 9(c) shows the final result after multiplying the projected areas by the relative probability.

A_SURF reveals the coarseness, or granularity, in the spacecraft model and debris threat in the GEOMETRY analysis. The default of 45 threat directions in BUMPER gives only 22 velocities due to symmetry. This will produce gaps along the velocity axis. "Waves" on the surface are an artifact of the coarseness of the modelling. The sphere is an easy shape to analyze since it looks the same from any direction. (That is why it is a separate option in the AREA_Maker macro.) The projected area from any direction is shown in Fig. 10. Also shown is its appearance if it were modelled using facets that cover 15 degrees of curvature. The granularity, or waviness is obvious.

The sphere is also a good representation of the surface area of any spacecraft that is not Earth oriented. It will appear to be randomly tumbling to the debris flux and average out to the oblique impacts on a sphere with the same surface area.

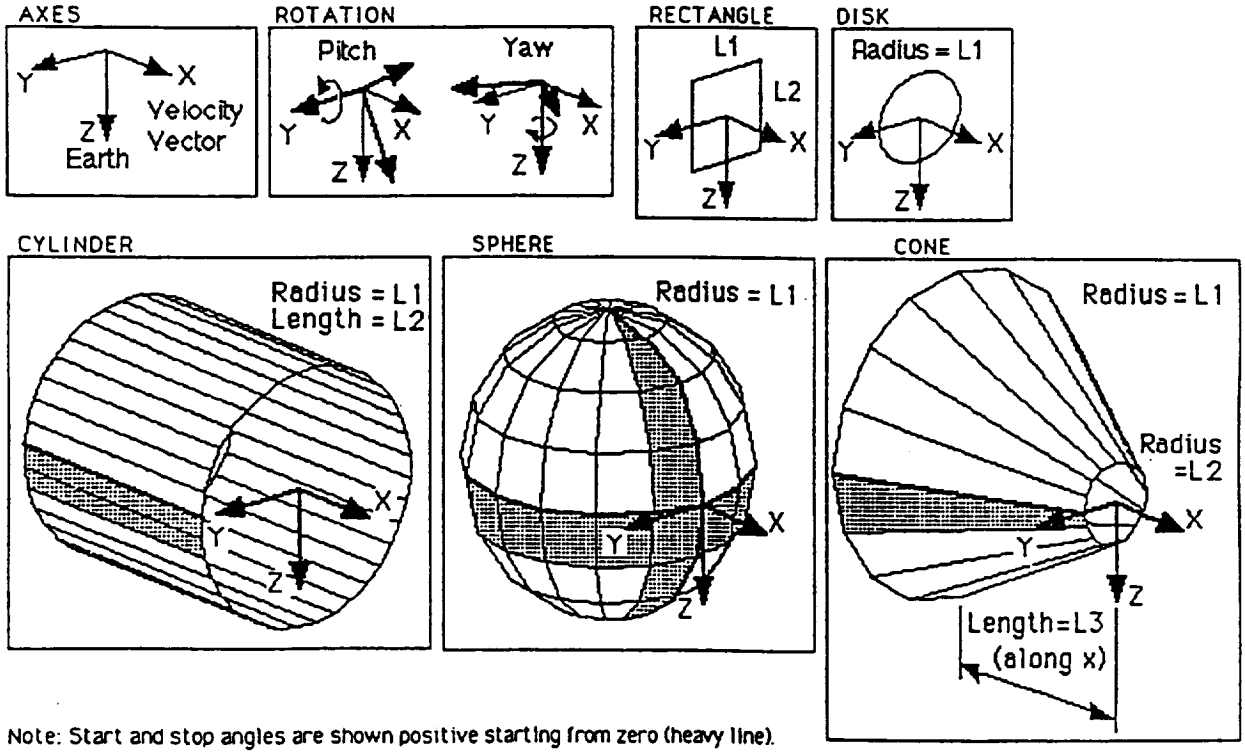

Note: Start and stop angles are shown positive starting from zero (heavy line).
Negative numbers may be used. (Eg. -90 to 90 for +y side of cylinder.)
Cone and cylinder are not symmetric. 0° to 5° does not also generate 175° to 180°.
The difference in the start and stop angles must be evenly divisible by the increment.

Fig. 8 AREA_MAKER Available Geometries

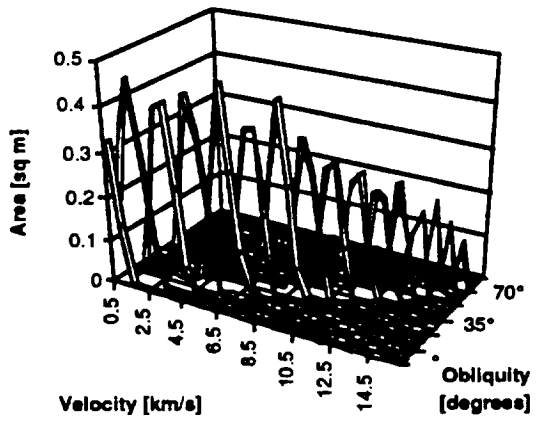

a) Projected areas in each threat direction.

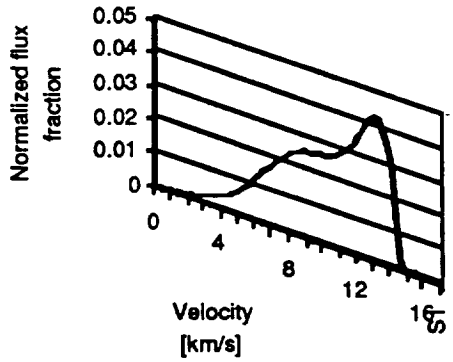

b) Probability distribution (as in Fig. 2.)

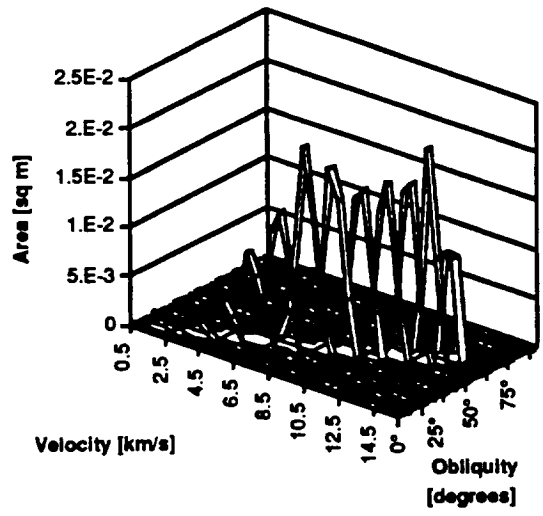

c) Effective area at each velocity and obliquity.

Fig. 9 AREA_MAKER analysis of a plate edge on to the direction of flight. (The surface normal is in the y axis in Fig. 8.)

Since the distributions are not smooth, the analyst must recognize that adjacent cells all with moderately high impact rates can be more significant than a single cell with the maximum impact rate.

Penetration Analysis

Figure 11 shows the P_SURF analysis of the effective area in Fig. 9. This is an example of the text-based contour plot. The ballistic limit was the RESPONSE output for a 0.050 inch bumper, four inch standoff, MLI, and a 0.125 inch 2219 aluminum rear wall, using the BUMPERII regression equation and default analysis of Wilkinson momentum failure.

Figure 12 is an illustration of the velocities and obliquities for which most penetrating impacts could occur on one early concept for a space station module. (The same RESPONSE ballistic limit surface is used as in the previous example.) It can be noted that BUMPER analyzed the PNP for one year as 99.88305%, while P_SURF calculated it as 99.88475%. The effective area was identical. But, as mentioned previously, partitioning the area to discrete velocities and obliquities will affect the result, just as assuming a curved surface is represented by a flat facet. The probability of penetration (POP = 1 - PNP) was 0.11695% for BUMPERII to 0.11525% for P_SURF. The percent change between the two is 1.5% of the POP.

Critical Damage Analysis

Mathematically the calculations for the probability of no critical damage (PNCD) are no different from the PNP calculations except that a critical damage surface is used instead of the ballistic limit surface for penetration. Use of the previously described critical damage limits gives a

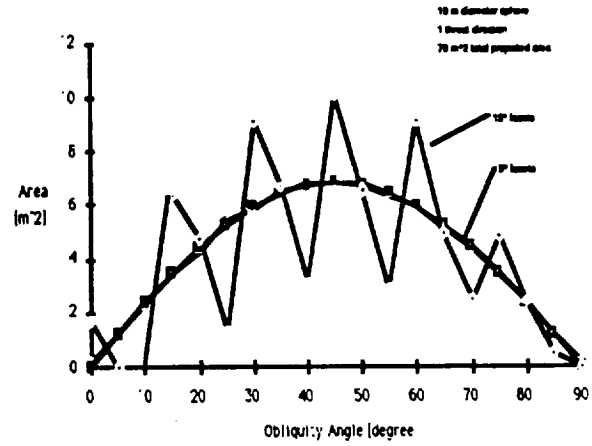

Fig. 10. Analysis of a sphere.

penetration of the baseline design, but collision

References

1. Coronado, A. et al.: "Space Station Integrated Wall Design and Penetration Damage Control," Contract NAS 8-36426, NASA-Marshall Space Flight Center, 1987.
2. Graves, Russel: BumperII User's Manual.
3. Elfer, N.; et al. Martin Marietta IR&D M-01S, unpublished research, 1987.
4. "Space Station Program Natural Environment Definition for Design," NASA SSP 30425.
5. Elfer, N.; and Rajendran, A. M.: "Space Debris Protection," in T. Wierzbicki, N. Jones Eds. *Structural Failure,* John Wiley & Sons, New York, p. 41-78, 1989.